Determination of Interspin Distances between Spin Labels Attached to Insulin: Comparison of Electron Paramagnetic Resonance Data with the X-Ray Structure

Heinz-Jürgen Steinhoff,* Nicole Radzwill,* Wilhelm Thevis,# Volker Lenz,# Dietrich Brandenburg,# Alfred Antson,§ Guy Dodson,§ and Axel Wollmer‖

*Lehrstuhl für Biophysik, Ruhr-Universität Bochum, 44780 Bochum, #Deutsches Wollforschungsinstitut an der Rheinisch-Westfälischen Technischen Hochschule Aachen, 52062 Aachen, and ‖Institut für Biochemie, Rheinisch-Westfälische Technische Hochschule Aachen, 52057 Aachen, Germany; and §Protein Structure Research Group, Department of Chemistry, University of York, Heslington, York, United Kingdom

ABSTRACT A method was developed to determine the interspin distances of two or more nitroxide spin labels attached to specific sites in proteins. This method was applied to different conformations of spin-labeled insulins. The electron paramagnetic resonance (EPR) line broadening due to dipolar interaction is determined by fitting simulated EPR powder spectra to experimental data, measured at temperatures below 200 K to freeze the protein motion. The experimental spectra are composed of species with different relative nitroxide orientations and interspin distances because of the flexibility of the spin label side chain and the variety of conformational substates of proteins in frozen solution. Values for the average interspin distance and for the distance distribution width can be determined from the characteristics of the dipolar broadened line shape. The resulting interspin distances determined for crystallized insulins in the R6 and T6 structure agree nicely with structural data obtained by x-ray crystallography and by modeling of the spin-labeled samples. The EPR experiments reveal slight differences between crystal and frozen solution structures of the B-chain amino termini in the R6 and T6 states of hexameric insulins. The study of interspin distances between attached spin labels can be applied to obtain structural information on proteins under conditions where other methods like two-dimensional nuclear magnetic resonance spectroscopy or x-ray crystallography are not applicable.

INTRODUCTION

The knowledge of a protein's structure is a basic requirement for understanding its function. X-ray structure analysis and two-dimensional nuclear magnetic resonance (NMR) spectroscopy have provided deep insight into the structure-function relationship of various proteins and nucleic acids. However, due to unresolved problems of crystallization and the lack of high-resolution NMR data, the determination of structures of membrane proteins is still a challenge. This is also true for the solution structures of water-soluble proteins or associates of high molecular weight. An alternative method to obtain structural information with a time resolution in the millisecond time range is based on the electron paramagnetic resonance (EPR) spectroscopy of spin-labeled macromolecules. Recently, a combination of EPR and genetic techniques was successfully introduced in this research field, namely, the site-directed spin labeling (SDSL) (Hubbell and Altenbach, 1994). Here, a natural amino acid is exchanged for a cysteine residue, which then will be spin labeled. This technique allows spin labels to be attached and studied at almost any desired site of a protein. SDSL with a single label specifically attached to a protein was applied to study secondary and tertiary structures of membrane proteins such as rhodopsin and bacteriorhodopsin (Hubbell and Altenbach, 1994), and to follow structural changes during their reactions (Shin et al., 1993; Steinhoff et al., 1994; Rink et al., 1997). In the present study additional progress in EPR application is described that allows distances between protein-bound spin labels to be determined.

The attachment of more than one spin label to a macromolecule with an interspin distance of less than ~2.5 nm leads to considerable EPR spectral changes, which are due to dipolar interaction. This dipolar interaction is in turn a measure of the interspin distance. In the past, various approaches have been made to obtain information on this dipolar interaction, which may allow an estimate of interspin distances in macromolecules of chemical or biological interest. The width and the intensity of the half-field signals in a powder spectrum were shown to yield distance information within the range of ~0.4–1.1 nm (Eaton et al., 1983). Peak height ratios and second moments of EPR spectra of dinitroxyls or line width measurements on spin-labeled peptides and proteins in frozen glass were shown to allow distance determination within the range of 1.0–2.2 nm (Likhtenshtein, 1976; Steinhoff et al., 1991; Rabenstein and Shin, 1995; Farahbakhsh et al., 1995; Farrens et al., 1996). In addition, perturbation calculations on EPR spectra with interacting spins and their comparison with experimental spectra provide the determination of the orientation of the interspin vector in the above mentioned distance range (Eaton and Eaton, 1989; Park and Trommer, 1989).

Received for publication 21 February 1997 and in final form 16 September 1997.

Address reprint requests to Dr. Heinz-Jürgen Steinhoff, Lehrstuhl für Biophysik, Ruhr-Universität Bochum, 44780 Bochum, Germany. Tel.: 49-234-7004463; Fax: 49-234-7094238; E-mail: hjs@bph.ruhr-uni-bochum.de.

0006-3495/97/12/3287/12 $2.00

The aim of the present study is to provide a method to determine intramolecular distances and distance distributions in proteins based on the measurement of the dipolar interaction of two attached spin labels. Special attention will be paid to the fact that proteins in solution are dynamic molecules distributed within a variety of conformational substates. Due to the conformational fluctuations and the possible flexibility of the spin-labeled side chains, the interspin distance and the relative nitroxide orientations in the frozen state may be distributed around average values. Simulated dipolar broadened EPR spectra are fitted to the experimental spectra, and the mean distance as well as the width of the distance distribution between the attached spin labels is calculated from the fitted line width function. The method is applied to different conformations of spin-labeled insulins. As a test, the EPR data determined for crystallized insulin in the R6 and T6 structures are compared with the x-ray structure of the spin-labeled samples.

MATERIALS AND METHODS

Spin labeling

The synthesis of spin-labeled insulins (Brandenburg et al., 1994) will be described in detail elsewhere (W. Thevis, V. Lenz, and D. Brandenburg, in preparation).

$N^{\alpha B1}$ -(2,2,5,5-tetramethyl-3-carboxy-pyrrolidin-1-oxyl)-insulin (B1SL)

$N^{\alpha A1}$,$N^{\varepsilon B29}$-bis-methylsulfonylethyloxycarbonyl-insulin (Msc_2-insulin) was acylated at B1-phenylalanine (cf. Fig. 1) with in situ generated hydroxybenzotriazole ester of carboxyproxyl. After deprotection under basic conditions, the crude product was purified by gel filtration, reverse-phase (RP) middle-pressure chromatography, and finally ion exchange chromatography. The purity according to RP high pressure liquid chromatography (RP-HPLC) was 94%.

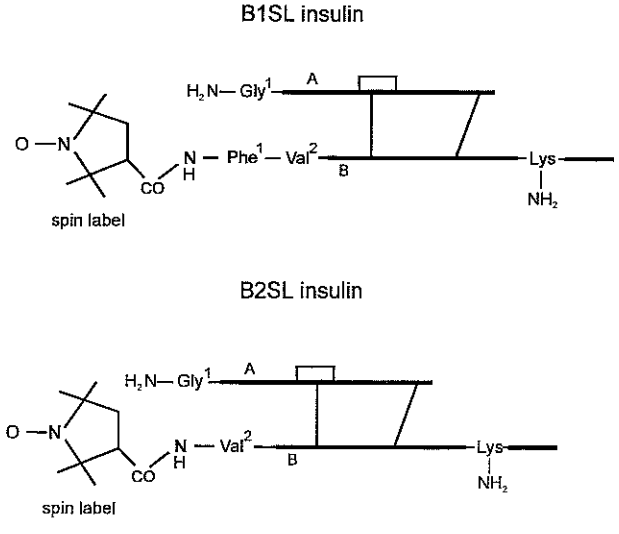

FIGURE 1 Structure of the proxyl group and simplified structure of insulin with the amino acid residues involved in modification and temporary protection. In B1SL, the proxyl group was attached to B1-phenylalanine. In B2SL, it was attached to B2-valine after removal of phenylalanine by Edman degradation.

$N^{\alpha B2}$ -(2,2,5,5-tetramethyl-3-carboxy-pyrrolidin-1-oxyl)-des-Phe^{B1}-insulin (B2SL)

B1-phenylalanine was cleaved from Msc_2-insulin by Edman degradation, i.e., reaction with phenylisothiocyanate and subsequent treatment with trifluoroacetic acid. The resulting protected des-PheB1-insulin was acylated, deprotected, and purified as outlined above. RP-HPLC showed a double peak with identical areas (total = 90%), indicating partial resolution of the R,S stereoisomers.

X-ray crystallography

Crystals of insulin labeled at the B-chain amino terminus (B2SL) were prepared using the established protocol to produce the 2Zn insulin form (T6) and the 2Zn phenol insulin (R6) (Fig. 2) (Baker et al., 1988; Derewenda et al., 1989). The T6 crystals that are rhombohedral proved to be very fragile and they diffracted poorly; no useful diffraction data have been recorded from these crystals. The R6 crystals belong to the monoclinic space group P21 with the cell dimensions of a = 47.97 Å, b = 61.53 Å, c = 60.77 Å, and β = 112.2°. The cell constants are comparable to those of the native crystals: a = 47.95 Å, b = 61.71 Å, c = 61.36 Å, and β = 110.8°.

The monoclinic crystals of the spin-labeled insulin are isomorphous to the native monoclinic insulin, which contains one insulin hexamer in the asymmetric unit (Derewenda et al., 1989). The two zinc ions are on the three-fold axis and each dimer traps two phenol molecules in their region of contact. In the R6 hexamer the B-chain residues B1–B8 continue as a helix from the central B9–B19 helical segment, Fig. 2 *b* and *c*.

Diffraction data were collected on a RAXIS IIC image plate detector, mounted on an RU200 Rigaku rotating anode x-ray generator operating at 50 kV and 100 mA, utilizing a graphite monochromator. The data extended to 2.3 Å spacing and showed good agreement between equivalents measurements (overall merging R-factor of 7.7%). Refinement of the native coordinates (initially excluding B1–B3) was carried out with these diffraction data using restrained least-squares minimization and Fourier map procedures (Collaborative Computational Project, 1994). The target restraints used were 0.02 Å for bond distances and 0.03 Å for angular distances. At convergence, the crystallographic agreement factor ($R = (\Sigma| |F_O| - |F_C| |/\Sigma |F_O|)$) was 17.9% for all data between 10 and 2.3 Å spacing and the root mean square (rms) deviations were 0.015 Å from ideal bond distances and 0.038 Å from angular distances. In addition to the protein atoms, 2 Zn^{2+} and 2 Cl^- ions and also 229 water molecules were included in the refinement calculations.

The crystallographic refinement revealed that the structure had relatively high thermal parameters particularly at the B-chain amino-terminal residues, which contain the spin label moiety. It was not possible to build the carboxy-proxyl group in chains D, F, and H accurately, and only approximate estimates for their positions are possible. For chains B, J, and L, the density is clear although it is a little diffuse (Figs. 2 *c* and 3). The atomic coordinates for the spin label groups have consequently an estimated error of ~0.2 Å .

Modeling of the B1SL-T6 structure was performed using the programs INSIGHT II and DISCOVER (Biosym, San Diego, CA). B1-phenylalanine was deleted from the native T6 structure (Baker et al., 1988), and the spin label was attached to B2. The orientation of the nitroxide was adjusted to mainly fill the space that was occupied by B1 before. Torsions about the spin label single bonds were performed to prevent overlap of nitroxide atoms with atoms of the protein. Thus, several slightly different starting configurations were constructed and energy minimization procedures were performed. The two configurations with the lowest energy (16 kcal/dimer and 36 kcal/dimer) revealed a distance between the nitroxides of closest approach of 10 and 13 Å, respectively, between the two spin labels in chains B and H, in chains F and L, and in chains J and D (cf. Fig. 2a). The

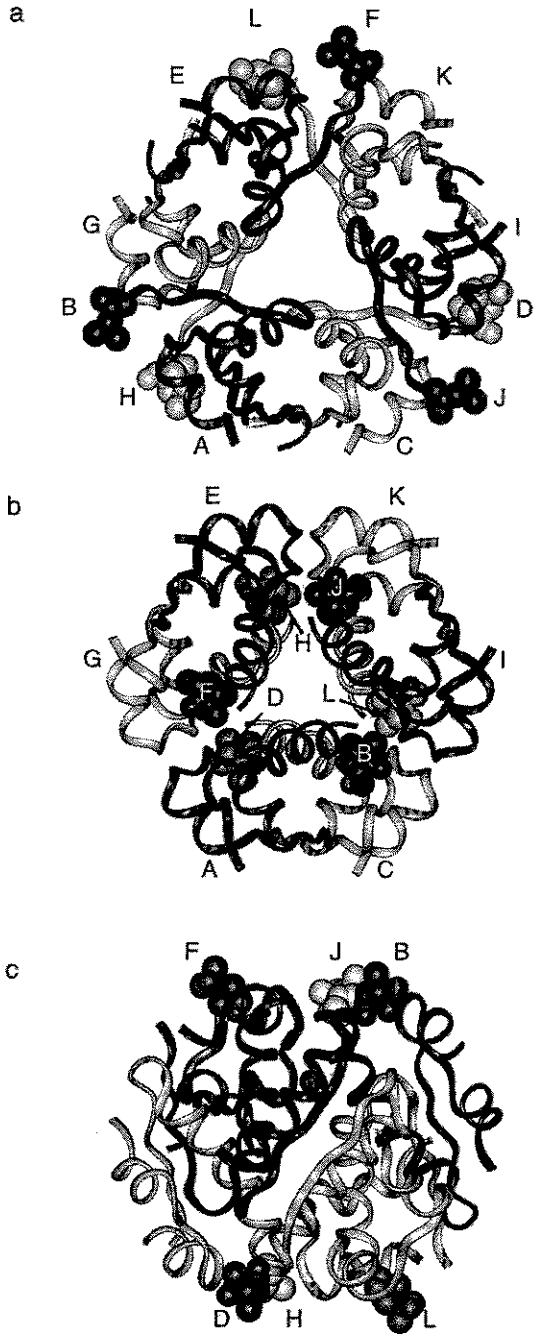

FIGURE 2 The B2SL insulin hexamer (*a*) in the T6 state and (*b*) in the R6 state as seen along the three-fold axis. The strands show the peptide backbone of the chains labeled A through L; the spin labels attached to the B-chains labeled B, D, F, H, J, and L are plotted space filled. The Zn ions and the phenols that stabilize the R6 structure are omitted. The electron spin probes are seen on the hexamer surface organized as two sets of trimers. For the T6 state, the respective spin probe positions were modeled; x-ray data of the spin labeled hexamers reveal the structure of the R6 state. The three poorly defined spin probe moieties were generated by symmetry operation from their well defined equivalents. After this operation, the generated coordinates were seen to sit sensibly in the low-level electron density. (*c*) A view of the B2SL insulin hexamer in the R6 state with the three-fold axis vertical. Here, the Zn ions are shown as spheres; they lie on the three-fold axis and are ~1.5 nm apart.

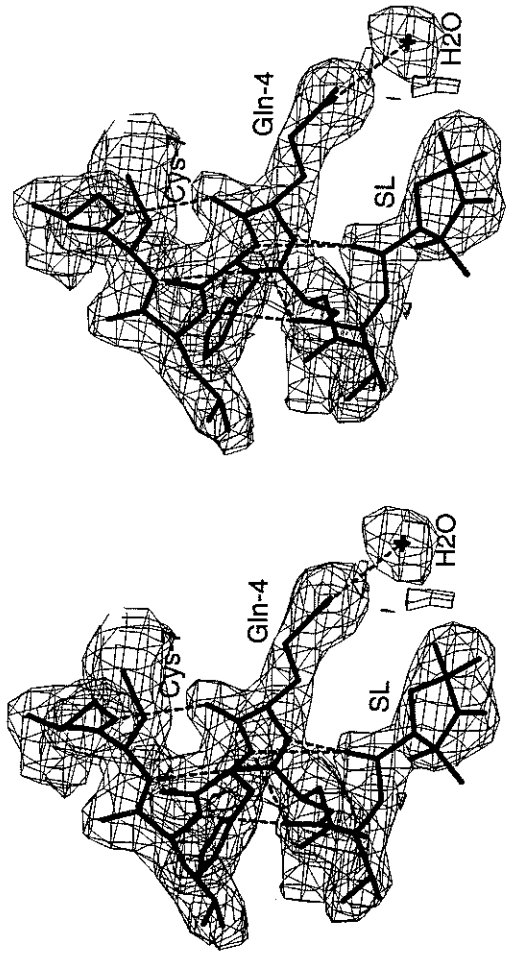

FIGURE 3 The electron density map calculated with coefficient $2|F_O| - |F_C|$ at the completion of the refinement. It is contoured at a level of 1 σ. The figure shows the residues B7 to the amino-terminal probe and a water molecule hydrogen bonded to B4 glutamine.

distance between the nitroxides attached to the B-chains within a dimer (chains B and D) exceeds 33 Å.

EPR measurements

Insulin solutions were prepared in 0.025 M Tris/HCl buffer, pH 7.8, at 10 mg/ml. A concentrated solution of $ZnSO_4$ was added up to a molar ratio of 0.33 metal ion/insulin monomer. The transition from the obtained T6 to the R6 structure was performed by the addition of a concentrated phenol solution to yield a final phenol concentration of 20 mM (Wollmer et al., 1987; Jacoby et al., 1993). The samples were loaded in EPR quartz capillaries. EPR spectra were recorded with a home-made X-band EPR spectrometer equipped with an AEG H_{103} rectangular cavity and a modified Oxford ESR 9 variable-temperature accessory. The magnetic field B_0 was measured with a Bruker B-NM 12 B-field meter. Spectra were recorded with a modulation frequency of 52 kHz and a modulation amplitude of 1.5 G. The microwave power was varied between 25 μW and 0.5 mW depending on the sample type. At the maximal used microwave power of 0.5 mW, line broadening due to saturation was found to have negligible effects on the distance determination for samples with interspin distances of <15 Å. Half-field experiments were performed with a modulation amplitude of 8 G. The forbidden transition in triplet systems does not show evidence of saturation below 200 mW (Eaton et al., 1983), thus a microwave power of 126 mW was used for the measurements of the half-field

spectra. After analog to 16 bit digital conversion, the spectra were processed in a personal computer.

EPR spectra simulations

In frozen solution, the diffusive residual motion of protein side chains is strongly restricted for temperatures below 200 K. The dynamics of proteins in this temperature regime exhibits glass-like behavior, and the rotational correlation time of spin label side chains exceeds 100 ns (Steinhoff et al., 1989). Only fast vibrational motions with very small amplitudes of the attached nitroxide ring are detectable (Steinhoff et al., 1989; Steinhoff and Karim, 1993). The residual averaging of the g- and hyperfine anisotropy is found to reduce the apparent hyperfine splitting by less than 2%. Thus, the EPR spectral line shape of a frozen protein solution or polycrystalline sample is adequately described by a powder spectrum. The shape of a powder spectrum of nitroxide spin labels randomly oriented in space is simulated on the grounds of the eigenvalues of the spin Hamiltonian:

$$H = \beta_e \mathbf{S}\mathbf{g}\mathbf{B}_0 + \mathbf{S}\mathbf{A}\mathbf{I} \tag{1}$$

where B_0 is the external magnetic field vector, β_e the Bohr magneton, S and I are the electron and the nuclear spin operators, respectively, $\mathbf{g}$ is the electron g value tensor, and $\mathbf{A}$ is the electron nuclear hyperfine tensor. The eigenvalues of the Hamiltonian are given to a good approximation by (Libertini and Griffith, 1970)

$$\begin{aligned} E &= g(\theta, \varphi)\beta_e B_0 M_S + A(\theta, \varphi) M_S M_I \\ g(\theta, \varphi) &= g_{xx} l_{zx} + g_{yy} l_{zy} + g_{zz} l_{zz} \\ A(\theta, \varphi) &= (A_{xx}^2 l_{zx} + A_{yy}^2 l_{zy} + A_{zz}^2 l_{zz})^{1/2} \end{aligned} \tag{2}$$

where g_{ii} and A_{ii} are the principle values of the tensors $\mathbf{g}$ and $\mathbf{A}$, respectively, and l_{zi} are the squared direction cosines between the nitroxide molecular axes i and the magnetic field directions z. M_S and M_I are the eigenvalues of S_z and I_z, respectively. The EPR line positions are calculated from Eq. 2 in steps of 3° for θ and ϕ. The intensity $I\, d\Omega$ of each absorption line is proportional to the number of molecules dN with their z molecular axis pointing into the space angle $d\Omega$. The intensity is given for a random distribution of nitroxide orientations by

$$Id\Omega \propto \sin\theta d\theta d\varphi \tag{3}$$

The procedure described above yields a stick spectrum that is convoluted by a superposition of a Gaussian and a Lorentian to account for the natural line-broadening mechanisms. Here, the line width is assumed to be independent of the orientation of the nitroxides. By means of a nonlinear least-squares fitting procedure the initially chosen values of g and A and the three line width parameters, the widths of the Gaussian and the Lorentian and the respective fractions, are varied iteratively until a minimum of the squared differences between experimental and simulated spectra is obtained. This method was extensively tested at X- and K-band frequencies for protonated and deuterated spin labels attached to proteins and was found to yield excellent agreement between experimental and simulated powder spectra (Steinhoff, 1988).

Dipolar broadening

The dipolar interaction of two unpaired electrons leads to considerable line broadening when motional averaging effects are absent. As discussed above, this is the case in the temperature regime below 200 K. The absorption lines of a pair of interacting spins are shifted from the points without interaction by the amount of ΔB, which is given to a good approximation by (Ciecierska-Tworek et al., 1973; Likhtenshtein, 1976)

$$\Delta B = \pm \frac{3g\beta_e(3\cos^2\theta - 1)}{4\rho^3} \tag{4}$$

where θ is the angle between the magnetic field B_0 and the distance vector ρ between the two interacting spins. Here, the effect of anisotropic magnetic tensors is neglected. The resulting dipolar line shape function $G(\Delta B)$ is calculated using Eq. 4 with discrete steps for θ of 3°. In a frozen solution or powder sample, the orientation distribution of the distance vector between the interacting spins may be assumed to be isotropic. Thus, the line intensity for each angle interval is determined from Eq. 3. To account for a range of distances expected to arise from a distribution of conformations of the protein or of the spin label side chain, a Gaussian distribution of interspin distances with a mean distance $\bar{r}$ and width σ is permitted. The assumption of a Gaussian distance distribution is justified below. The EPR spectrum $F(B)$ is calculated by convoluting the noninteracting spectrum $f(B)$ with the line shape function $G(\Delta B)$ (Steinhoff et al., 1991):

$$F(B) = \int f(B')G(B - B')dB' \tag{5}$$

Fig. 4 shows a set of EPR spectra simulated for different interspin distances ρ and distance distribution widths σ. Spectral parameters were chosen close to values found for the used spin label (Fig. 1) in aqueous glycerol solution. The simulated EPR line width significantly increases when the interspin distance becomes less than 2 nm (Fig. 4 *a*). The variation of σ changes the

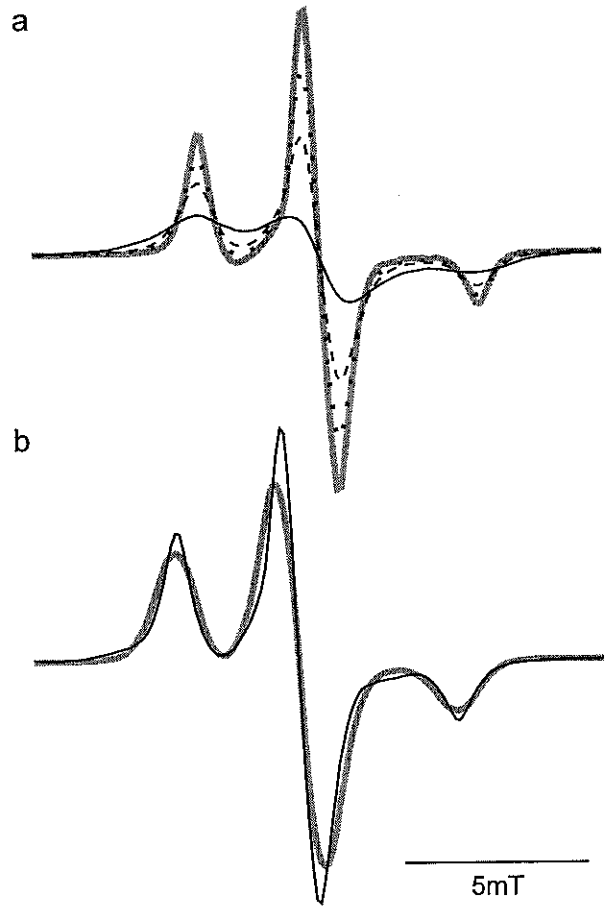

FIGURE 4 (a) Simulated EPR powder spectra for different interspin distances, ρ, and fixed ratio ρ/σ = 2.6, ρ = 1.0 nm (*thin line*), 1.4 nm (*dashed line*), 1.8 nm (*dotted line*), and 3.0 nm (*thick line*). (*b*) Simulations performed for a fixed average distance, ρ = 1.4 nm, and different distribution widths, σ, of 0.1 nm (*thick line*) and 0.9 nm (*thin line*). The spectra are normalized to constant spin number.

shape of the line-broadening function in a characteristic way, which is different from a simple mean distance variation (cf. Fig. 4 *b*).

When the interspin distance becomes very small, the electron orbitals overlap and the EPR line shape is modulated due to J coupling. A separation between line shape effects due to dipolar interaction and exchange interaction seems to be difficult for immobilized samples. However, if we take the values reported by Closs and co-workers (1992) as a first approximation for our systems, the exchange interaction frequency J falls below the value of the dipolar splitting for interspin distances larger than 10 Å. The present analysis is thus restricted to distances exceeding 10 Å, and additional experimental evidence will be given in the Results and Discussion that within this limit the analysis of only dipolar interactions is reasonable and practical.

Interspin distance distribution function

In a solution of spin labels, the nitroxides are uniformly distributed. The law of distribution of the nearest neighbor in a random distribution of particles is given by Chandrasekhar (1943)

$$w(r) = \exp(-4\pi r^3 n) 4\pi r^2 n \qquad (6)$$

where $w(r)$ is the probability of finding a particle within the distance range r and $r + dr$ and n is the particle density. The average interspin distance between nearest neighbors is calculated from this relation to

$$\bar{r} = 0.554 n^{-1/3} \qquad (7)$$

To facilitate a comparison of interspin distances of systems with different particle distributions it seems to be practical to express the distance distribution functions in terms of a Gaussian. Fig. 5 *a* shows a superposition of the probability function, Eq. 6, and a fitted Gaussian. With exception of the distance range below 0.5 nm the agreement between the Gaussian and Eq. 6 is nearly perfect. The value of $\bar{r}$ extracted from the fitted Gaussian deviates less than 1% from the true value given by Eq. 7. The ratio of the mean distance $\bar{r}$ to the width σ of the Gaussian was found to yield 2.64. For the distance range below 0.5 nm the effect of the residual discrepancy between both functions is negligible for our study; the distance of closest approach between the nitroxides is set to 0.6 nm during the spectra simulations to account for the finite nitroxide dimension.

To analyze the shape of the distance distribution function for protein-bound spin labels, molecular dynamics simulations on R6(B1SL) insulin were performed. The determination of the distance distribution requires the characterization of the entire space accessible to the nitroxide rings. To perform this task within reasonable computation time, stochastic simulations at high temperature were performed according to the method described by Steinhoff and Hubbell (1996). The GROMOS (Biomos, Groningen, The Netherlands) program package was used. Each of the B-chains of the insulin trimer in the R state was modified by attachment of a nitroxide side chain to amino acid position 1. After energy minimization, all amino acids outside a sphere of 1.5 nm around the nitroxide nitrogen were deleted. Thus, the total number of atoms was reduced from 2500 to 765. Bond lengths and positions of the backbone atoms were constrained using the SHAKE (van Gunsteren and Berendsen, 1982) algorithm. After energy minimization, the backbone atoms, with the exception of those of the first four amino acids of the B-chain, were fixed and the system was first equilibrated at 100 K and then heated up to 300 K and finally to 600 K. From a trajectory of 1.6 ns length, the distances between the nitrogen atoms of neighboring nitroxides were extracted. The distance distribution is shown in Fig. 5 *b*. For distances exceeding the distance of closest approach, 0.6 nm, a Gaussian is found to adequately fit the simulated distance distribution function. The fitting reveals a value for the mean distance $\bar{r} = 1.64$ nm and a half-width $\sigma = 0.62$ nm. A Gaussian was also found to fit the interspin distance in spin-labeled lysozymes (Steinhoff et al., 1991). We conclude that a Gaussian is a good approximation for the distance distribution function of uniformly distributed nitroxides and for flexible spin label side chains attached to proteins.

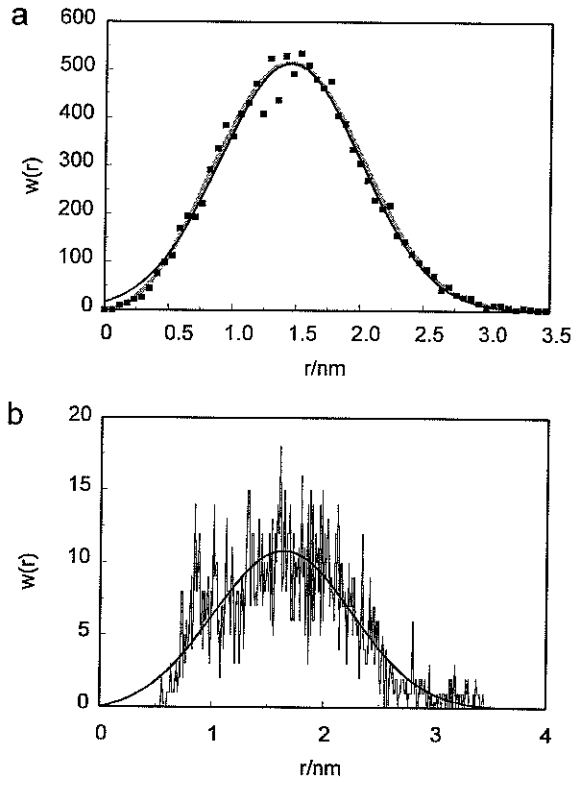

FIGURE 5 (*a*) Distribution of the distance between nearest neighbors for a simulation of 12,000 particles distributed uniformly in solution. The probability to find a particle in the distance range $r + \Delta r$, $w(r)$, is plotted versus r with the particle density set according to a concentration of 100 mM (■). The behavior of $w(r)$, calculated from Eq. 6, fits the simulated data well (*thick line*). A Gaussian (*thin line*) is superimposed with its maximum at $r = 1.45$ nm and a width of 0.56 nm. (*b*) The distance distribution function $w(r)$ for spin labels attached to B1 of insulin hexamers in the R6 state determined from a molecular dynamics simulation in vacuum. The superimposed Gaussian reveals an average distance of 1.64 nm and a distribution width, σ, of 0.62 nm.

RESULTS

Interspin distances of nitroxides in frozen solution

Nitroxide spin labels dissolved in glycerol-water mixtures are an appropriate model system for which an isotropic interspin distance distribution and an independent isotropic orientation distribution of the nitroxides can be assumed. To prevent motional averaging of the anisotropic magnetic interactions the samples were frozen in a 60% glycerol-water glass. Comparison with spectra measured at 80 K shows that temperatures below 200 K were found to be sufficient to provide the powder spectral shape of immobilized nitroxides. Fig. 6 *a* shows the experimental EPR spectrum of 1-oxyl-2,2,6,6,-tetramethylpiperidine (TEMPO) recorded at 170 K and a superimposed simulated powder spectrum with the fitted values of the tensors **g** and **A**, $g_{xx} = 2.0088$, $g_{yy} = 2.0062$, $g_{zz} = 2.0021$, $A_{xx} = 7.1$ G, $A_{yy} = 6.6$ G, $A_{zz} = 37.4$ G. The line-broadening function is composed of 74% Gaussian of a width of 4.3 G, and 26%

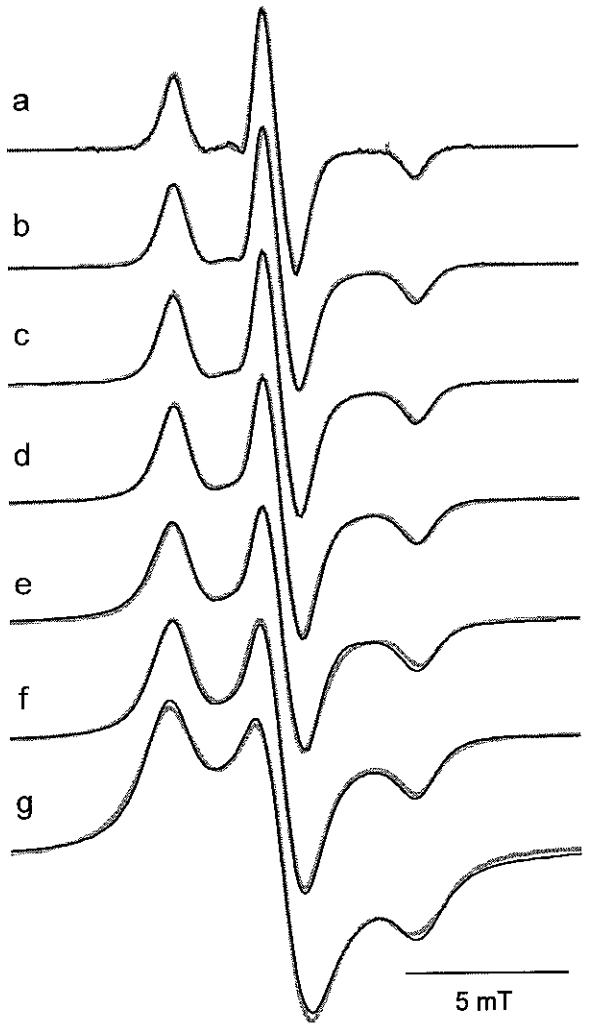

FIGURE 6 EPR spectra of TEMPO spin label in frozen glycerol water solution for different spin label concentrations: (*a*) 0.005 M; (*b*) 0.05 M; (*c*) 0.08 M; (*d*) 0.1 M; (*e*) 0.15 M; (*f*) 0.2 M; and (*g*) 0.3 M. The thick lines are fits of simulated EPR powder spectra. Adjustable parameters in (*a*) were the values of the g- and A-tensors and the line width parameters; no dipolar interaction was included. In the simulations shown in (*b*)–(*g*) these values were fixed and the distance ρ and the distribution width σ were adjusted.

Lorentian of a width of 4.3 G. The excellent agreement between experiment and simulation, as well as the comparison of the fitted values of the tensor elements with the powder values (cf., e.g., Steinhoff et al., 1989) strongly argue for an immobilization of the nitroxides on the EPR time scale. After increasing the nitroxide concentration, a considerable increase of the line width is observed (Fig. 6 *b–g*). To fit the simulated spectra shown in Fig. 6, *b–g*, the values of the tensors **g** and **A** and the line width parameters were fixed corresponding to the values found for the diluted sample shown in Fig. 6 *a*, and the average distance ρ and the distance distribution width σ were adjusted. Again, the simulated EPR spectra agree with the experimental data (Fig. 6, *b–g*). The fitted average interspin distance ρ was plotted versus the average distance to the nearest neighbor, $\bar{r}$, calculated from the spin label concentration according to Eq. 7. The result is shown in Fig. 7. The values ρ agree with the values of $\bar{r}$ within the experimental error. The error bars include uncertainties of the nitroxide concentration. The small systematic deviation between the values of $\bar{r}$ and ρ may result from neglecting the dipolar influence of the next nearest neighbor. From the simulation of 12,000 randomly distributed particles (distance distribution given by the data points shown in Fig. 5 *a*), the ratio of the distances to the nearest neighbor and to the next nearest neighbor is found to be 1:1.5. Due to the ρ^{-3} dependence of the dipolar broadening effect (cf. Eq. 4), the influence on the line shape is small. It is equivalent to a maximal decrease of the effective ρ of 10%, which explains the observed deviation.

The characteristics of the ratio ρ/σ is determined from the spectra simulations in the distance range from 1.0 to 1.6 nm. The values are obviously independent of the average distance to the nearest neighbor as shown in Fig. 7. The mean value yields $\rho/\sigma = 2.6$, which agrees with the theoretical value extracted from the distribution function, Eq. 6, $\bar{r}/\sigma = 2.64$ (cf. Fig. 5 *a*). For distances >1.6 nm, the effect of the dipolar broadening on the spectral shape is very small, and a meaningful value for σ can be extracted only from signals with optimized signal to noise ratio.

The above study demonstrates that the application of the method to samples with a random distribution of nitroxides yields reasonable values for the average interspin distance ρ and for the distance distribution parameter σ in the range of 1.0 to ~2.0 nm.

Interspin distances in spin-labeled B1SL and B2SL insulins determined from EPR experiments

To determine the magnetic and line width parameters in the absence of dipolar interaction, an insulin sample was pre-

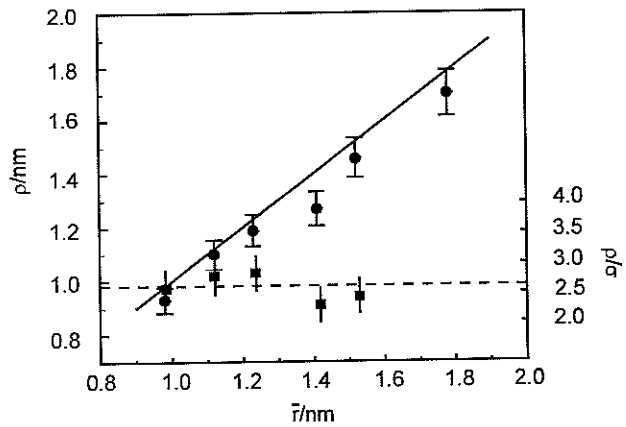

FIGURE 7 The fitted values of the interspin distance ρ (●) and of ρ/σ (■) for the samples shown in Fig. 6, *b–g*, plotted versus the average distance to the nearest nitroxide neighbor, $\bar{r}$, calculated from Eq. 7. The full line shows the function $\bar{r} = \rho$, and the dashed line is the average value of $\rho/\sigma = 2.6$. For interspin values exceeding 1.8 nm no reasonable values for σ could be fitted due to the very small dipolar broadening of the spectra. In this case σ was fixed to $\rho/2.64$.

pared with a ratio of spin-labeled to unlabeled monomers of 1:5. The insulin concentration and solution conditions were adjusted to yield hexamers in the T6 conformation (see Materials and Methods). The EPR spectra of this diamagnetically diluted sample and of the completely labeled insulin hexamers in the R6 and T6 conformations are shown in Fig. 8 *a*. Compared with the diamagnetically diluted sample, a considerable dipolar broadening in the completely labeled samples is revealed by the increase of the spectral amplitude close to the first relative minimum as a consequence of the increased line width. The dipolar line broadening is similar for the B1SL and B2SL samples in the T6 conformation in solution. The dipolar interaction of the spin labels in the R6 conformation of B1SL is considerably stronger than that in B2SL. Compared with the protein samples in solution, the dipolar interaction is increased in the crystal state of B2SL in the T6 conformation. The contrary is true for the R6 conformation. An increase of the dipolar interaction in the crystal state may be due to a different structure of the protein with a decreased interspin distance compared with that in solution or to an interaction between spin labels attached to different hexamers. However, the decrease of the dipolar interaction found in the crystal structures of R6(B2SL) must be caused by different structures of the amino termini in the crystal and in solution.

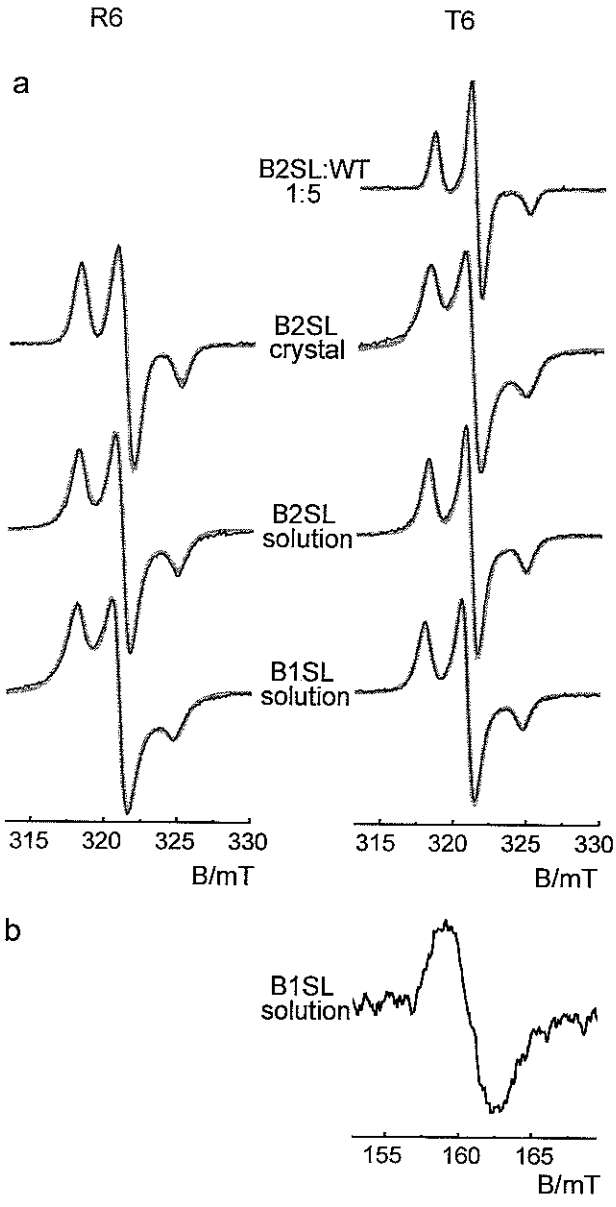

FIGURE 8 (*a*) EPR spectra of spin-labeled insulin hexamers in glycerol water glass at 170 K. The thick lines are fits of simulated EPR powder spectra with the interspin distance ρ and the distribution parameter σ as adjustable parameters. The fitted values are shown in Table 1. (*b*) Half-field spectrum (T = 80 K) of 6 mM T6(B1SL). The relative intensity of the half-field transition to the allowed transition for this sample was 2.5×10^{-5}.

To determine the interspin distances, we assume that the main contribution to the dipolar broadening comes from pairs of interacting spin labels. On this assumption, the average interspin distance ρ and the distribution parameter σ were fitted. The spectral simulations are superimposed on the experimental data and shown in Fig. 8 *a*, and the values of the fitted parameters are given in Table 1. As can be seen, there is an excellent agreement between the simulations and the experimental spectra.

Due to the location of the amino termini of the B-chains in the R6 hexamer (see Fig. 2), an interaction model consisting of three equally spaced spins agrees better with the molecular structure in solution than an interaction model of pairs of spins. For a system with three interacting spin labels, the dipolar spectral line shape is estimated from the simple pair model (see Materials and Methods), which is expanded in a classical way; the magnetic field resulting from two magnetic dipoles located at positions ρ_1 and ρ_2 with respect to a third nitroxide are calculated for the four combinations of the dipole orientations using Eq. 4. Spectra that were fitted according to this model correspond almost exactly to those calculated from the pair model. However, the fitted interspin distance is increased by 25% compared with that of the pair model in order to match the experimental spectral shape. The interspin distance values for the R6 structure calculated using this model are shown in Table 1.

The distribution widths σ are smallest for the crystallized samples and increase to approximately twice this value for the hexamers in solution (cf. Table 1). This is a reasonable result because the amino terminus is expected to be more structured in the crystal state, whereas a number of protein conformations with slightly different orientations of the chain termini may exist in solution. Studies on the mobility of the B-chain amino terminus in crystal and solution will be described below.

For comparison, the relative intensity of the half-field transition was determined for the T6 conformation of B1SL. As the transition probability of the forbidden half-field transition is low, high protein concentrations were necessary to provide reasonable signal to noise ratios. The spectrum of a sample of 6 mM protein concentration is shown in

TABLE 1 Average distance and distance distribution, ($r \pm \sigma$)/nm, between nitroxide nearest neighbors determined by EPR dipolar interaction analysis and x-ray crystallography

	R6(B2SL)		R6(B1SL)	T6(B2SL)		T6(B1SL)
	Crystal	Solution	Solution	Crystal	Solution	Solution
EPR	1.7 ± 0.3	1.4 ± 0.6	1.0 ± 0.6	1.1 ± 0.4	1.4 ± 0.6	1.3 ± 0.6
X-ray	1.8* (2.1#)			1.0§		

*Interspin distance between nitroxides of different hexamers.
#Interspin distance within three equivalent spin labels.
§Interspin distance estimated from the structure of the native protein with modeled spin labels.

Fig. 8 *b*. To separate contributions from inter- and intramolecular spin-spin interaction spectra of the half-field transition for sample concentrations of 16, 6, 4, and 2 mM were recorded. Extrapolated to infinite dilution the relative intensity yields 2.1×10^{-5}, which corresponds to an average interspin value $\langle r^{-6} \rangle^6 = 1.0$ nm (Eaton et al., 1983). As the relative intensity of the forbidden transition depends on r^{-6}, the average is weighted in favor of molecules with smaller values of r. A Gaussian distribution of the interspin distance with the mean value of 1.3 nm and distribution width of 0.6 nm found for T6(B1SL) (see Table 1) yields $\langle r^{-6} \rangle^6 = 0.96$ nm, which is in nice agreement with the result of the half-field experiment.

Interspin distances in B2SL insulin hexamers determined from x-ray crystallography

The spin-labeled hexamer crystal was isomorphous to the native R6 insulin crystal. The atomic parameters for the protein atoms, except for the three amino-terminal B-chain residues, were taken from the native structure and refined by restrained least-squares minimization. The residues B1–B3 were excluded from the refinement as their conformation was liable to be affected by the attached spin label. At convergence, difference Fourier maps were calculated, which revealed the positions for the excluded residues and the spin label. The electron density for all six equivalent B-chain amino-terminal residues was clear and showed that their conformations were essentially identical to those of the native hexamer. The spin label moiety was clear in only three of the six B-chains in the hexamer. It was possible in these cases to determine the conformation at the probe satisfactorily (Fig. 3). The probe moiety has approximately the same conformation in all three cases with the largest deviations from the average structure of less than 0.3 Å. In these cases, reasonably accurate coordinates were determined and refined. In the other three cases, the diffuse and low-level electron density indicated that the spin labels were poorly ordered. However, although the atomic positions could not be accurately determined, it was possible to position the moieties sensibly using the noncrystallographic symmetry. Comparison of the three equivalent spin labels showed that they were approximately in the same position relative to the amino-terminal helix. Fig. 2 *c* shows the hexamer viewed side-on with the probe moieties space filled.

The interspin distance within the three equivalent spin labels B, F, and J (cf. Fig. 2 *b*) as determined from this crystal structure amounts to 2.1 nm. The distance to the nitroxide nitrogen of the nearest spin label in the other trimer (D, H, and L) of the same hexamer is 3.9 nm. Thus, due to the $1/r^3$ dependence of the dipolar splitting, the EPR line broadening for dissolved hexamers is expected to be dominated by the interaction of the three equivalent spins within a trimer. In the crystal, however, the distance of one of these nitroxides to the next nitroxide of the nearest hexamer is 1.8 nm. Thus, the application of the above model of three interacting spins (B-F-G, D-H-L) on the analysis of the crystal spectra will lead to an underestimation of the nitroxide distances.

In contrast to that, the distance between the nitroxide groups of the spin labels in the T6 conformation is shortest for the B-chains of two different trimers, i.e., between chains B and H, F and L, and J and D (cf. Fig. 2 *a*) and amounts to 1.0 nm. The distance to the next nearest N-O neighbor within the same hexamer is 3.3 nm and to the nearest hexamer in the crystal is 1.5 nm. Thus, the dipolar broadening is assumed to be essentially determined by pairs of spin labels with an interspin distance of 1.0 nm. The interspin distances that essentially determine the dipolar broadening are included in Table 1.

Characterization of the spin label environment in terms of the spin label side chain mobility

At temperatures below 200 K, protein fluctuations, including the spin label residual motion, are frozen (Steinhoff et al., 1989). The distribution parameter σ determined from the dipolar broadening may be taken as a measure for the distribution width of possible configurations of the amino termini of the B-chain. These different configurations are due to the flexibility of either the spin label side chain or of the binding site environment or of both. At room temperature, the spin label side chain motion occurs in the nanosecond time range, and the nitroxide mobility and the flexibility of the peptide backbone are directly reflected in the EPR absorption line shape (Miick et al., 1991, 1993; Steinhoff and Hubbell, 1996). The room temperature spectra of the R6 and T6 conformations of B1SL and B2SL insulin are shown in Fig. 9. In the crystal structures, the mobility of the nitroxide side chain is reduced, as can be concluded from the spectral line shape. The dipolar interaction between

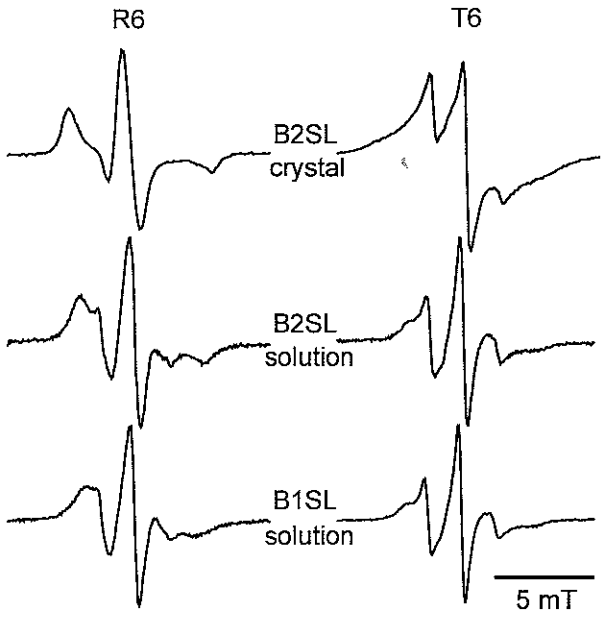

FIGURE 9 EPR spectra of spin-labeled insulin hexamers at room temperature (T = 293 K) in the crystal state and in solution in both conformations, T6 and R6. Due to residual motion of the spin labels in the crystal and in solution at room temperature, the anisotropy of g and the hyperfine interaction as well as the electron dipolar interaction are partially averaged.

neighboring spins is not completely averaged, as is revealed by the long wings of the low-field and high-field lines of the spectra of B2SL in the T6 structure. However, even the protein structure in the crystal allows for small-amplitude residual motion of the nitroxide side chain as can be seen from the comparison of the spectra of B2SL at 293 K and at 170 K. Especially for the T6 structure, a mobile component is revealed by the small splitting of the resolved low- and high-field peaks, which are superimposed on the dipolar broadened powder-like spectrum.

The solution spectra of the T6 and R6 states of B1SL insulin and B2SL insulin are very similar, respectively. Now the dipolar interaction is averaged due to the rotational diffusion of the protein and the residual motion of the spin labels. The spectra of the T6 state show multi-component lines in the low- and high-field regions. These lines may be caused by an anisotropic residual motion of the nitroxide or by at least two conformations of the amino terminus of the B-chain that may lead to different spin label mobilities. EPR spectra simulations (Freed, 1976) were performed to estimate effective reorientation correlation times of the nitroxides on grounds of isotropic Brownian diffusion. Best fits were obtained with a superposition of two spectra simulated with effective correlation times of 7 and 1.6 ns. The slow component contributes to more than 80% as determined from double integration of the simulated single spectra. For the insulin hexamers in the R6 conformation, effective correlation times were estimated at 4 ns for B1SL and 5 ns for B2SL with the shorter terminus.

The application of the Stokes Einstein law with the average radius of the insulin hexamer determined from the crystal structure yields a rotation correlation time of 10 ns in water at 298 K. In all cases, the experimentally determined values are smaller and thus demonstrate the presence of a residual motion of the nitroxide. Despite different local environments of the spin labels in the B1SL and B2SL samples due to the different lengths of the amino termini, the spectra are very similar. This indicates that more amino acid residues than those of the amino terminus are involved in this residual motion. The x-ray data of the T6 structure of the native insulin support this finding. The temperature factors of the B-chain residues show a steep increase from the fifth to the first position (Baker et al., 1988). Thus, different residual mobilities of the B-chain amino termini in the different structures are here revealed in solution by the EPR spectra.

DISCUSSION

The accurate determination of intramolecular distances and distance changes in proteins is crucial for the understanding of functional mechanisms. High-precision methods are required in combination with straightforward chemistry and data analysis. Recent progress in site-specific spin labeling makes the EPR spectroscopy a promising tool for analyzing systems of biological interest (Hubbell and Altenbach, 1994). The method presented here is based on the fitting of simulated EPR spectra to experimentally determined spectra of spin-labeled proteins. The degree of dipolar interaction between two spin labels attached to specific sites of the protein provides the information about intramolecular distances and distance distributions.

In simulating the dipolar broadening, a number of approximations are made. First, the distribution of the angle between the interspin vector and the external magnetic field is expected to be isotropic. This is certainly true for most biological systems in solution and for polycrystalline samples. Second, for a given interspin vector, the molecular orientation of the nitroxide ring is assumed to be isotropic owing to the degree of rotational freedom of the protein molecules along the interspin vector and to the flexible link between the nitroxide ring of the spin label and the protein. In turn, this residual flexibility of the nitroxide and a possible structural flexibility of the protein require the consideration of an interspin distance distribution. Theoretical considerations and molecular dynamics simulations reveal that the interspin distance distribution function for spin labels uniformly distributed in frozen solution or attached to proteins may be approximated by a Gaussian.

The experimental evaluation of the dipolar broadening as a measure of the interspin distance requires freezing of the nitroxide motion to avoid averaging of the dipolar interaction. The temperature dependence of the protein dynamics in frozen aqueous solution appears to be similar to that of glasses with the glass transition close to 200 K (Frauenfelder et al., 1988). The residual motion of protein-bound spin labels was found to behave according to this model

(Steinhoff et al., 1989, 1993). The reorientation correlation time of the diffusion-like motion of the attached nitroxides exceeds 100 ns and thus is completely quenched on the EPR time scale for temperatures below 200 K. The residual averaging of the hyperfine interaction detected in the temperature range from 70 K to 200 K, which changes the effective hyperfine splitting by less than 2% in frozen solution, is attributed to fast oscillations of very small amplitude of the nitroxide ring atoms. As all measurements of the dipolar interaction were done at temperatures below 200 K, we conclude that motional averaging effects on the dipolar splitting are negligible.

When the interspin distance becomes very small, the electron orbitals overlap and the EPR line shape is modulated due to J coupling. The magnitude of J, or the singlet-triplet splitting, is determined by contributions from through-space interaction and coupling through the σ bonds of the molecule. Through-bond coupling decreases exponentially with the number of σ bonds between the labels. In the present protein samples, the nitroxides belong to different peptide chains, thus coupling through bonds should be absent. The through-space value of J, however, has to be taken into account for interspin distances of less than ~10 Å. Here, exchange interaction frequency J approaches the value of the dipolar splitting if we take the values reported by Closs and co-workers (1992) as a first approximation for our systems. A separation between line shape effects due to dipolar splitting and J coupling seems to be very difficult for immobilized samples. Thus, the present analysis is restricted to interspin distances exceeding 10 Å.

The analysis of the EPR spectra shows that the above assumptions are well justified for the case of free spin labels in glycerol-water glass measured at 170 K. The fit of a simulated powder spectrum to the diluted sample reveals effective hyperfine tensor elements that do not show any evidence for motional averaging. Distances and distance distribution widths are extracted from the EPR spectra in a distance range between 1.0 and 1.8 nm within an error of less than 5%. The simulated spectra agree with the experimental data. No significant systematic deviation of the extracted distance values from the expected ones are observed over the total distance range (cf. Figs. 6 and 7). This suggests that the effect of exchange interaction on the experimental spectra is negligible even for distances in the range of 1 nm. For distances above 1.5 nm the determination of the distribution width σ is difficult because the dipolar line broadening becomes much less than the intrinsic line width of the continuous wave spectrum. Due to this reason, the uncertainty for the average interspin distance will also increase for distance values exceeding 1.8 nm. The use of deuterated spin labels may expand the upper distance limit because of their property of reducing the intrinsic line width.

The most important test of the method is the comparison of distance data determined from EPR experiments in spin-labeled proteins with their x-ray structures. Hexameric insulin provides two well studied conformations with different distances between the amino termini of the B-chains, the R6 and the T6 conformations. For spin labels attached to B2SL, the distances in the protein crystals are determined by x-ray analysis and EPR spectroscopy. For the R6 state, the spin pair with the closest approach between the two nitroxides shows an interspin distance of 1.8 nm, and the largest distance to a nearest neighbor does not exceed 2.1 nm. The EPR analysis yields an interspin distance of 1.4 ± 0.3 nm on the assumption that the interaction between spin pairs is sufficient to account for the total dipolar line broadening and 1.7 ± 0.3 nm for the model of three interacting spins. These models lead to an underestimation of the distance values as soon as the interaction between more than two or three spin labels contributes significantly to the line width. This is true if the distance to the next nearest neighbor is less than 2 nm as for the spin labels in the crystallized R6 structure. Thus, the interspin distance of 1.7 nm has to be understood as a lower limit.

However, the pair interaction model holds for the T6 state, where the spin-spin interaction between the spin label of the pairs B-H, J-D, and F-L (cf. Fig. 2 *a*) within a single hexamer by far dominates other possible dipolar contributions. From the atomic data of the modified native crystal structure an interspin distance of 1.0 nm was estimated for the structure of lowest energy. In agreement with this, the analysis of the dipolar broadening yields an interspin distance of 1.1 ± 0.4 nm. The comparison between x-ray data and EPR results demonstrates that the EPR method for the intramolecular distance determination can successfully be applied for pairs of interacting spins; for proteins or assemblies with more than two interacting spin labels the pair model may be used to estimate a lower limit of the interspin distances.

Distance determinations in frozen solution were performed with insulin samples spin labeled at positions B1 or B2. In this case, only dipolar interactions within a single hexamer have to be considered. Compared with the R6 crystal state, the dipolar interaction in frozen solution is increased, but the contrary is true of the T6 state (cf. Fig. 8 *a*). The model of a trimer of equally spaced spins was used to simulate the EPR spectra of the R6 state and the pair model was used for the T6 samples. Again, excellent agreement is obtained between simulation and experiment (cf. Fig. 8 *a*) and reasonable distance values could be determined. Measurements of the ratio of the intensity of the forbidden half-field transition to the intensity of the allowed transition support the values of ρ found for T6(B1SL). This intensity ratio was shown to be independent of the exchange coupling constant J (Eaton et al., 1983). The agreement between the results of both methods again justifies that exchange effects on our spectra in the distance range above 1.0 nm were neglected.

The decrease of the interspin distance in B2SL in the R6 conformation in solution compared with that of the crystal state reveals that the positions of the amino termini of the B-chains are closer to each other, i.e., closer to the threefold axis of the hexamer. This conclusion is supported by

the distance values determined for B1SL. The extension of the B-chains by one residue decreases the average distance between the amino termini from 1.4 to 1.0 nm (cf. Table 1). A movement of each amino terminus by ~0.2 nm toward the poles of the hexamer caused by the additional residue accounts for these data. The addition of a single residue within an α-helix increases its length by 0.14 nm, whereas the length of an extended chain would be increased by 0.32 nm. The measured displacement of 0.2 nm agrees well with the above limits and suggests an arrangement of the amino termini oriented toward each other in the solution structure of R6.

As is the case in R6, the location of the B-chain amino termini in the T6 structure in solution differs from that in the crystal. The introduction of the probe at B1 or B2 will prevent the B-chain amino terminus to be buried completely, as is seen in the native T6 2Zn insulin hexamer (Baker et al., 1988). The distance between neighboring B-chain amino termini of different trimers is increased by ~0.3 nm in solution compared with that in the crystal, probably because the lattice packing ties down B8–B5. The B1SL structure reveals distance values close to those of the B2SL structure.

Slight differences between solution and crystal structures of proteins are well known from comparisons between data determined by NMR spectroscopy and x-ray crystallography. The location of the amino termini are additionally determined by inter-hexamer contacts in the crystal. In solution, the nitroxide environment is different, and therefore, the amino termini may occupy a number of different orientations. In addition, the chain termini are expected to be more flexible in the dissolved protein than in the crystallized sample. The different flexibility is reflected in the distance distribution parameter σ, which is significantly smaller for the crystallized than in the dissolved samples. The degree of the nitroxide mobility is determined from EPR spectra of the crystallized and dissolved proteins at room temperature. In both cases, R6 and T6, the nitroxides are immobilized in the crystal by the interaction with nearby structure. In solution, the nitroxides are fairly mobile. The nitroxide mobility is different for the R6 and T6 structures with the highest motional restrictions sensed in the T6 state. Strikingly, the spectra of B1SL and B2SL reveal very similar mobilities of the spin labels in the respective structures. This suggests that the motional freedom of the amino terminus mainly determines the EPR spectral shape rather than the residual motion of the nitroxide ring. In a well structured hexamer, B1SL and B2SL may be expected to be different, because of their different local environment. The absence of a significant difference indicates that the amino termini in T6 and R6 are released from the hexamer to a similar extent. In both, T6 and R6, this is easy to understand. In T6, the modified B1 and B2 residues cannot pack into the hexamer. In the native R6 molecule, B1 and B2 are exposed and therefore both are very mobile; modification by the probe will lead to similar mobilities. Approximately 80% of the protein molecules in the T6 structure are found with an amino terminus more immobilized than that in the R6 structure.

Several different methods for distance measurements between nitroxides have been developed and applied in the past. In the motional narrowing regime, the dipolar interaction tensor averages to zero and J coupling determines the EPR spectral shape for interspin distances of less than 1 nm. The determination of J provides relative distances and thus allows the analysis of the secondary structure of doubly spin-labeled peptides (Miick et al., 1992; Fiori et al., 1993; Hanson et al., 1996). Second moment calculations and measurements of peak height ratios, which were empirically calibrated using different nitroxide biradicals, were suggested to study interspin distances in immobilized proteins in the range from 1 to 2 nm (Likhtenshtein, 1976). Using a Fourier deconvolution technique, the dipolar interaction of spin labels attached to α-helical peptides was determined and shown to be applicable as a molecular ruler in the distance range from approximately 0.8 to 2 nm (Rabenstein and Shin, 1995). Half-field intensity measurements of immobilized samples allow distances measurements in the range up to 1.2 nm without interference due to possible exchange interaction (Eaton et al., 1983). If the relative positions of the nitroxide groups are fixed in a static position and not affected by dynamic processes of the protein, the dipolar interaction results in the splitting of the hyperfine lines into two new peaks on either side of the original EPR spectrum. In this case, the line shapes and positions of the split peaks of dipolar spectra are sensitive to the distance and to the relative orientations of the nuclear hyperfine tensors (Park and Trommer, 1989; Eaton et al., 1983; Eaton and Eaton, 1989). However, proteins are dynamic systems, and in many cases, the nitroxide side chains are flexible. The degree of the flexibility depends on the length of the spin label side chain, on the strength of its interaction with atoms of adjacent secondary and tertiary structures, and on the distribution of conformational substates of the protein (Steinhoff and Hubbell, 1996). Due to this flexibility, the nitroxide orientations and spin label positions are distributed around average values in the frozen protein, where the fluctuation rates are strongly decreased. The present approach accounts for this effect and provides the distance distribution width in addition to the mean value. In the distance range between 1.0 and 1.2 nm the analysis of the dipolar broadened line shape has advantages compared with half-field experiments because the signal to noise ratio is more than three orders of magnitude higher. Thus, the investigation of spin-labeled protein mutants is possible, where the sample volume and the protein concentration might be limited. Due to this high sensitivity, distance measurements in the range up to 2.0 nm are possible. The use of deuterated spin labels with their smaller intrinsic line widths may expand this range. The exchange interaction frequency J was found to be negligible compared with the dipolar splitting for interspin distances exceeding 1 nm. This is in agreement with results of Rabenstein and Shin

(1995) who could neglect J coupling influences for interspin distances larger than 0.8 nm.

In summary, the method of analyzing EPR dipolar interaction is well suited to estimate interspin distances of spin-labeled proteins as demonstrated for a model system. In combination with the freeze quenching technique, time-dependent conformational changes of proteins might be followed. Using genetic engineering techniques, nearly any desired site of a protein can be spin labeled (Hubbell and Altenbach, 1994). Taking these experimental tools into account, the EPR dipolar interaction analysis method opens a wide field of investigating protein structures.

This work was supported by the Deutsche Forschungsgemeinschaft (Ste640/2–1, SFB394) (H.-J. Steinhoff). The generous support of the Juvenile Diabetes Foundation International (grant 193110) is gratefully acknowledged.

REFERENCES

Baker, E. N., T. L. Blundell, J. F. Cutfield, S. M. Cutfield, E. J. Dodson, G. G. Dodson, D. C. Hodgkin, R. E. Hubbard, N. W. Isaacs, C. D. Reynolds, K. Sakabe, N. Sakabe, N. M. Vijayan. 1988. The structure of 2Zn pig insulin at 1.5 Å resolution. *Philos. Trans. R. Soc. Lond. (Biol.)* 319:369–450.

Brandenburg, D., W. Thevis, D. Glasmacher, J. Pirrwitz, M. Fabry, E. Schaefer, and L. Ellis. 1994. Analysis of the interaction between insulin and its receptor by means of covalent and non-covalent techniques. *In* Peptides: Chemistry, Structure and Biology. R. S. Hodges and J. A. Smith, editors. Escom Science Publishers, Leiden, The Netherlands. 574–576.

Chandrasekhar, S. 1943. Stochastic problems in physics and astronomy. *Rev. Mod. Phys.* 15:1–89.

Ciecierska-Tworek, Z., S. P. Van, and O. H. Griffith. 1973. Electron-electron dipolar splitting anisotropy of a dinitroxide oriented in a crystalline matrix. *J. Mol. Struct.* 16:139–148.

Closs, G. L., M. D. E. Forbes, and P. Piotrowiak. 1992. Spin and reaction dynamics in flexible polymethylene biradicals as studied by EPR, NMR, and optical spectroscopy and magnetic field effects: measurements and mechanisms of scalar electron spin-spin coupling. *J. Am. Chem. Soc.* 114:3285–3294.

Collaborative computational project, number 4. 1994. *Acta Crystallogr. D.* 50:760–763.

Derewenda, U., Z. Derewenda, E. J. Dodson, G. G. Dodson, C. D. Reynolds, C. Sparks, and D. Swenson. 1989. Phenol stabilizes more helix in a new symmetrical zinc insulin hexamer. *Nature.* 338:594–596.

Eaton, G. R., and S. S. Eaton. 1989. Resolved electron-electron spin-spin splittings in EPR spectra. *In* Biological Magnetic Resonance 8: Spin Labeling Theory and Applications. L. J. Berliner and J. Reuben, editors. Plenum Press, New York. 339–397.

Eaton, S. S., K. M. More, B. M. Sawant, and G. R. Eaton. 1983. Use of the EPR half-field transition to determine the interspin distance and the orientation of the interspin vector in systems with two unpaired electrons. *J. Am. Chem. Soc.* 105:6560–6567

Farahbakhsh, Z. T., Q.-L. Huang, L.-L. Ding, C. Altenbach, H.-J. Steinhoff, J. Horwitz, and W. L. Hubbell. 1995. Interaction of α-crystallin with spin-labeled peptides. *Biochemistry.* 34:509–516.

Farrens, D. L., C. Altenbach, K. Yang, W. L. Hubbell, and H. G. Khorana. 1996. Requirement of rigid-body motion of transmembrane helices for light activation of rhodopsin. *Science.* 274:768–770.

Fiori, W. R., S. M. Miick, and G. L. Millhauser. 1993. Increasing sequence length favors α-helix over 3_{10}-helix in alanine-based peptides: evidence for a length-dependent structural transition. *Biochemistry.* 32: 11957–11962.

Frauenfelder H., F. Parak, and R. D. Young. 1988. Conformational substates in proteins. *Annu. Rev. Biophys. Biophys. Chem.* 17:451–480.

Freed, J. H. 1976. Theory of slow tumbling ESR spectra for nitroxides. *In* Spin Labeling I: Theory and Applications. L. J. Berliner, editor. Academic Press, New York. 53–132.

Hanson, P., G. Millhauser, F. Formaggio, M. Crisma, and C. Toniolo. 1996. ESR characterization of hexameric, helical peptides using double TOAC spin labeling. *J. Am. Chem. Soc.* 118:7618–7625.

Hubbell, W. L., and C. Altenbach. 1994. Investigation of structure and dynamics in membrane proteins using site-directed spin labeling. *Curr. Opin. Struct. Biol.* 4:566–573.

Jacoby, E., P. Krüger, Y. Karatas, and A. Wollmer. 1993. Distinction of structural reorganization and ligand binding in the T to R transition of insulin on the basis of allosteric models. *Biol. Chem. Hoppe Seyler.* 374:877–885.

Libertini, L. J., and O. H. Griffith. 1970. Orientation dependence of the electron spin resonance spectrum of di-*t*-butyl nitroxide. *J. Chem. Phys.* 53:1359–1367.

Likhtenshtein, G. I. 1976. Spin Labeling Methods in Molecular Biology. John Wiley, New York.

Miick, S. M., K. M. Casteel, and G. L. Millhauser. 1993. Experimental molecular dynamics of an alanine-based helical peptide determined by spin label electron spin resonance. *Biochemistry.* 32:8014–8021.

Miick, S. M., G. V. Martinez, W. R. Fiori, A. P. Todd, and G. L. Millhauser. 1992. Short alanine-based peptides may form 3_{10}-helices and not α-helices in aqueous solution. *Nature.* 359:653–655.

Miick, S. M., A. P. Todd, and G. L. Millhauser. 1991. Position-dependent local motions in spin-labeled analogues of a short α-helical peptide determined by electron spin resonance. *Biochemistry.* 30:9498–9503.

Park, J. H., and W. E. Trommer. 1989. Advantages of ^{15}N and deuterium spin probes for biomedical electron paramagnetic resonance investigations. *In* Biological Magnetic Resonance 8: Spin Labeling Theory and Applications. L. J. Berliner and J. Reuben, editors. Plenum Press, New York. 547–595.

Rabenstein, M. D., and Y.-K. Shin. 1995. Determination of the distance between two spin labels attached to a macromolecule. *Proc. Natl. Acad. Sci. U.S.A.* 92:8239–8243.

Rink, T., J. Riesle, D. Oesterhelt, K. Gerwert, and H.-J. Steinhoff. 1997. Spin-labeling studies of the conformational changes in the vicinity of D36, D38, T46, and E161 of bacteriorhodopsin during the photocycle. *Biophys. J.* 73:983–993.

Shin, Y.-K., C. Levinthal, F. Levinthal, and W. L. Hubbell. 1993. Colicin E1 binding to membranes: time-resolved studies of spin-labeled mutants. *Science.* 259:960–963.

Steinhoff, H.-J. 1988. A simple method for determination of rotational correlation times and separation of rotational and polarity effects from EPR spectra of spin-labeled biomolecules in a wide correlation time range. *Biochem. Biophys. Methods.* 17:237–248.

Steinhoff, H.-J., O. Dombrowsky, C. Karim, and C. Schneiderhan. 1991. Two dimensional diffusion of small molecules on protein surfaces: an EPR study of the restricted translational diffusion of protein-bound spin labels. *Eur. Biophys. J.* 20:293–303.

Steinhoff, H.-J., and W. L. Hubbell. 1996. Calculation of electron paramagnetic resonance spectra from Brownian dynamics trajectories: application to nitroxide side chains in proteins. *Biophys. J.* 71:2201–2212.

Steinhoff, H.-J., and C. Karim. 1993. Protein dynamics and EPR-spectroscopy: comparison of molecular dynamic simulations with experiment. *Ber. Bunsenges. Phys. Chem.* 97:163–171.

Steinhoff, H.-J., K. Lieutenant, and J. Schlitter. 1989. Residual motion of hemoglobin-bound spin labels as a probe for protein dynamics. *Z. Naturforsch.* 44c:280–288.

Steinhoff, H.-J., R. Mollaaghababa, C. Altenbach, K. Hideg, M. Krebs, H. G. Khorana, and W. L. Hubbell. 1994. Time-resolved detection of structural changes during the photocycle of spin-labeled bacteriorhodopsin. *Science.* 266:105–107.

van Gunsteren, W. F., and H. J. C. Berendsen. 1982. Algorithms for Brownian dynamics. *Mol. Phys.* 45:637–647.

Wollmer, A., B. Rannefeld, B. R. Johansen, K. R. Hejnaes, P. Balschmidt, and F. B. Hansen. 1987. Phenol-promoted structural transformation of insulin in solution. *Biol. Chem. Hoppe Seyler.* 368:903–911.